FURTHER DEVELOPMENT OF A CODE TO PREDICT FUNDAMENTAL MATERIAL AND FRACTURE PROPERTIES OF NUCLEAR GRAPHITE

Chris Lynch and Gareth B. Neighbour,
University of Hull, Cottingham Road, United Kingdom, HU6 7RX

Introduction

Polygranular graphite is used as a moderator, reflector and major structural component within the UK's Advanced Gas-cooled Reactors (AGR's) operated by British Energy plc. In recent times, cracking phenomena has occurred within the graphite bricks at an earlier stage than is to be expected. This project aims to increase the understanding of graphite crack propagation by modelling quasi-brittle fracture processes. This paper advances the model presented previously (see Lynch and Neighbour, 2006) by the inclusion of the mathematical algorithm "circles within circles" to develop complex pore structures. The model also contains an algorithm to model radiolytic oxidation in nuclear graphite. Thus, the new code, written in C++, currently predicts, in broad terms, the microstructure and mechanical properties of nuclear graphite with increasing radiolytic oxidation. The model also has the potential to model the effects of neutron irradiation simultaneously with radiolytic oxidation given a set of operating rules. This paper focuses on presenting a set of results from the modelling of porosity and radiolytic oxidation and comparing these results with the classical Knudsen relationship for nuclear graphite amongst other relationships.

Failure and the Complications of the Fracture Process

The quasi-brittle fracture response of polygranular graphite, illustrated in Figure 1, has been documented by Brocklehurst (1977), Sakai *et al.* (1983), Allard *et al.* (1991), Ouagne (2001), Fazluddin (2002) amongst others. Generally, pre-peak behaviour is associated with sub-critical cracking throughout the material, whilst, generally, post-peak behaviour is associated with microcracking ahead of the crack tip (process zone). The characterisation and prediction of the fracture process is very difficult due to a range of complex interactions which can be grouped into five main categories:

- Microstructure
- Crack / surface morphology
- Fracture process zone and sub-critical processes
- Scale
- Degradation (*e.g.* reduction in strength through oxidation)

Degradation is a major issue for nuclear graphite in-service within the reactor core. Radiolytic oxidation, due to the activation of the CO_2 coolant, attacks the graphite microstructure indiscriminately: initially through the open pore network (*e.g.* volatile gas evolution and transport pores) and then ultimately breaks through to the closed porosity (*e.g.* calcination cracks within the filler particles). For a detailed explanation on both neutron irradiation and radiolytic oxidation see Brocklehurst *et al.* (1970), Murdie *et al.* (1986) and Birch *et al.* (1990).

Knudsen Relationship

The Knudsen equation has a long history and is a widely used semi-empirical structure-property relationship, and has proved to be applicable to a wide range of materials (Rice, 1977) and is widely used for the prediction of the effects of oxidation on the graphite moderator in AGRs (Burchell *et al.*, 1985). Traditionally, the Knudsen relationship is used to predict the decline in a mechanical property with increasing weight loss, or more precisely, decreasing density. For example, it is common to describe the relationship between Young's modulus and oxidation of AGR moderator graphite by the equation

$$E/E_0 = \exp(-bx), \qquad\qquad [1]$$

where E is the Young's modulus of the graphite oxidised to a fractional weight loss x, E_0 is the Young's modulus of the unoxidised graphite and b is an exponent. For radiolytic oxidation, b = 3.7 ± 0.2 (±1 s.d.) whilst values for thermal oxidation range between 5 and 10 (Neighbour and Hacker, 2001). It is useful to note here that a physical basis for the equation is often given as a stacked array of solid spheres, and that the mechanical properties of this ideal material are controlled by the contact area between the stacked solid spheres. The resultant change in relative contact area between the spheres underpins the exponential response.
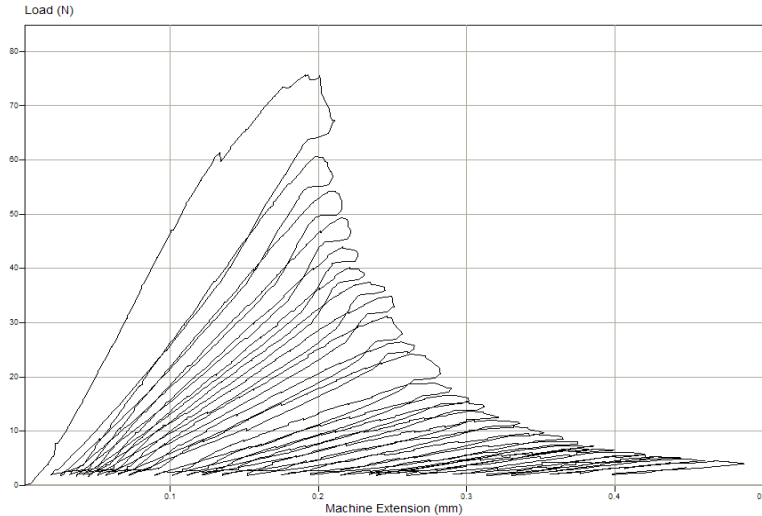

Figure 1: Cyclic load-displacement curve for AGR graphite (Chevron Notched Specimen) which shows stable crack growth and quasi-brittle characteristics.

Rice (1996a, b, & c) in reviewing the porosity dependence of physical properties of materials remarks that mechanical properties depend primarily on one basic characteristic of the pores, and thus this leads him to recommend the Minimum Solid Area approach, *i.e.* properties are based upon a solid cross-sectional area of the material (described below). As indicated in Figure 2, empirically, mechanical properties follow almost a universal trend plotted as the logarithm of the relative value of the property (P/P_0) versus the volume fraction porosity (p). There are three characteristics: (a) first a very near-linear region (*i.e.* closely following an e^{-bp} dependence where b is the slope); (b) then a region where the property decrease with increasing p accelerates, *i.e.* a roll-over in the property; and (c) the culmination of this rollover with the property precipitously decreasing to zero at a specific volume fraction, P_c, which is the percolation limit for the solid phase defining the particular porosity. As Rice (1996a, b & c) remarks there is substantial impact of processing / pore character on property-porosity relations. He further states that because of the complexity of the problem, and the resultant simplifying assumptions made to make the problem tractable, the "correctness" of the porosity models can only be determined from extensive comparison with data. An alternative to this approach is the computational abstract model proposed herein.

Minimum Solid Area

Given the suggested physical basis for the Knudsen equation, a useful concept to aid our understanding is the Minimum Solid Area (MSA) of a material. The MSA of a material can be defined as the minimum cross sectional area between pores normal to an applied uniaxial stress field. Consequently, the assumption being made is that MSA is proportional to the property in question, *e.g.* Young's modulus, E. To emphasise this approach, Rice (1996a, b & c) reports that semi-analytical derivations, commonly used to obtain E, are generally based on load-bearing area, *i.e.* using the fact that the elastic property is directly proportional to the average cross-sectional area of the solid material in planes normal to the stress. However, although the model is assumed, at least initially, to be an isotropic body, the model is two-dimensional and a correction needs to be applied. Actually, in the 2D case, it is the Minimum Line Length (MLL) that is important as shown in Figure 3.
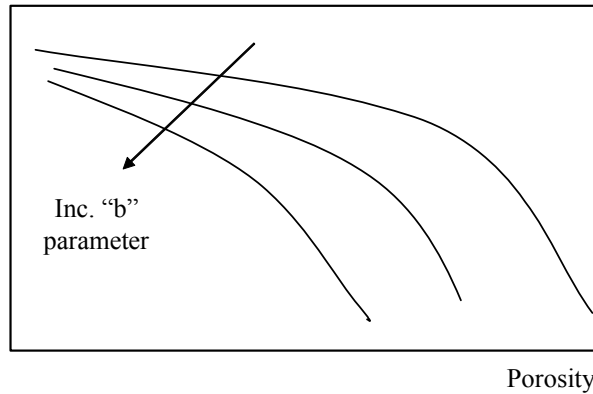
Ln Property

Inc. "b"
parameter

Porosity

Figure 2: A schematic of typical variation of natural logarithm of a property versus increasing porosity (the "b" parameter refers to the Knudsen relationship).
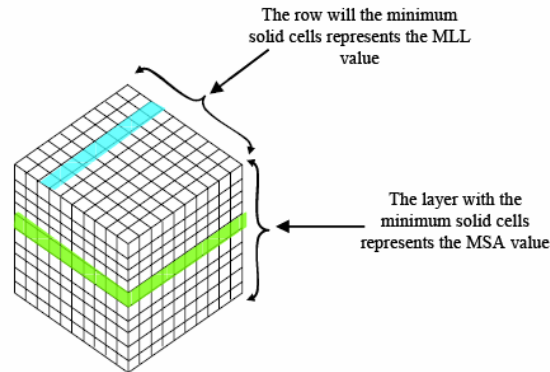

The row will the minimum
solid cells represents the MLL
value

The layer with the
minimum solid cells
represents the MSA value

Figure 3: An illustration of the relationship between the MSA and MLL.

Development of the Abstract Model

There are a number of methods of modelling the relationship between microstructure and the mechanical properties of brittle materials. As discussed, one of the more predominant methods is Minimum Solid Area (MSA). The classical MSA models assume that the pores do not interconnect and that there is a percolation limit where, due to the limits of packing regular geometric objects, it is no longer possible to increase the amount of porosity without interconnecting the pores. The Minimum Solid Area (MSA) provides the most appropriate explanation of the empirically found Knudsen relationship. The key question is the explanation of the exponent "b" and this is a key objective of this part of the code. The MSA is found to decay exponentially with increasing porosity for simple geometric models formed from the stacking of regular shaped voids. Therefore the change in MSA causes a relative change in material properties such as Young's modulus. The Knudsen equation is a type of MSA model (based upon the contact between solid spheres), and therefore it is possible to fit the Knudsen equation to MSA models and extract values for the decay parameter b. More importantly, establishing that the predicted value of b matches the experimental observation provides an important validation of the code.

In the development of any model, it is useful to start with a two-dimensional model and work up to a three dimensional model. In the case of the model here, special attention needs to be given to whether there are any peculiarities in doing this. To illustrate the point, first consider a two-dimensional version, as illustrated in Figure 3, in which the model consists of a lattice structure in which linear analysis can be carried out such as "rastering" down the structure interrogating the resultant image. The simple model used here is a spherical pore within a unit cell of length unity. The MSA of a spherical pore with a radius r, in a cubic unit cell is thus defined as $1-\pi r^2$ and the volume of

porosity is defined as $4/3\pi r^3$. That is to say, MSA is a two dimensional parameter obtained from a three dimensional model. Equally, if a two dimensional model is used, *i.e.* a circle within a square, correspondingly, the one-dimensional (equivalent to MSA but called here Minimum Line Length - MLL) for a circle with a radius r, in a square unit cell is defined as $1-2r^2$ and the area of porosity is defined as πr^2. As porosity increases, a similar trend is observed, but, initially at least, the 2D model is more pessimistic (see Figure 4); indeed it exhibits a more exponential behaviour than the MSA model. As can be seen from Figure 4, there are differences between the two models, with MLL showing greater exponential behaviour than MSA especially at low fractional porosities, though both models percolate at different fractional porosity; the worst case being the 3D model percolating at 0.55 which is a curiosity of the idealised system. Considering graphite as a material, it is hard to justify the representation of the microstructure by spherical pores, when the reality of the pore structure is a collection of complicated pore shapes and sizes, especially at high weight losses when large pores become interconnected by long thin sinuous pores. In summary, it is possible to suggest that if a material's MLL changes exponentially with porosity, then its MSA would change exponentially with porosity as well. The MLL is a two dimensional MSA model that also allows the application of MSA to pseudo-micrographs as would be done with real microstructures and image analysis. By normalisation, any analysis can relate the predicted / measured Young's modulus results with the theoretical MLL results derived for each pseudo-microstructure generated. Taking the approach further, the results of any model will be heavily influenced by the shape of porosity. The least detrimental to mechanical properties is that of a rectangle, aligned parallel to the applied stress axis. The most detrimental pore geometry is that of an ellipse, aligned perpendicular to the applied stress axis.
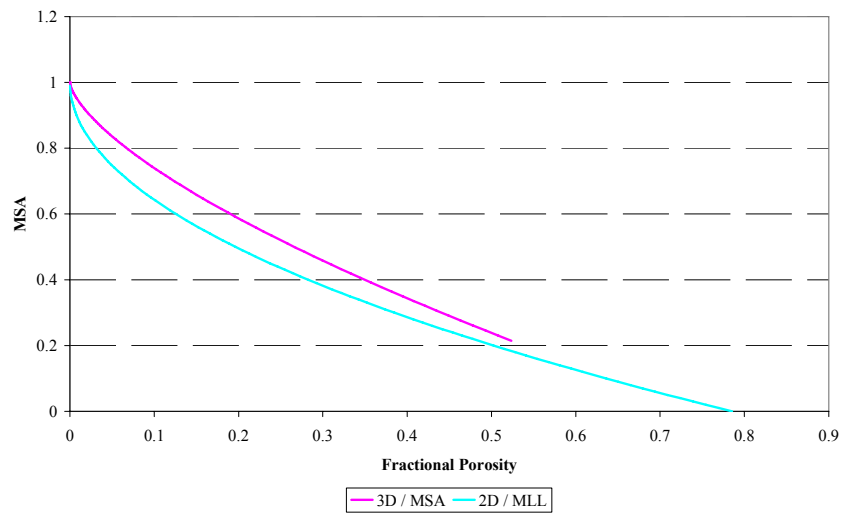

Figure 4: Relationship between the MSA and MLL approaches for a simple spherical pore within a solid matrix.

The Model

The model is split into five components: user interface; microstructure; degradation; fracture; and outputs (graphical and data). Each of the components although independent of one another, in terms of code, has a hierarchal dependency meaning that their inputs rely upon the previous component during the execution process. The nature of the dependencies and the way in which they are carried through to all the components means that the critical part of the code is the first component, the microstructure.

User Interface
Currently, the user interface for inputting values is a basic window very similar to that used by the windows command prompt and MS-DOS (Microsoft Disk Operating System). This keeps memory usage to a minimum and also provides clear instructions for input.

Microstructure

As mentioned, the microstructure component of the code is critical because all the components following in the execution process use the values created during runtime by this component. This core component is responsible for the creation of the base structure used throughout all subsequent calculations. In the simplest form, the component uses a two dimensional dynamic array of integers (representing different microstructural features), which is held in the computer's memory. The use of a dynamic array is critical and thus allows complex algorithms to be used. Each cell in the array has a byte size associated with it, in this case each cell = 2 bytes of memory for a short integer so a two dimensional array of 10 x 10 = 100 cells would result in a total memory of 200 bytes. Each cell within the array equates to a physical size of 1 micron. The main inputs into the code (and thus the microstructure) are initial "as-received" pore size distribution, Figure 5; particle size distribution & shape factors; constituents (filler, "binder" and porosity); starting porosity; and, the level of radiolytic oxidation. It is important to note that the model would otherwise be a simple geometric construction without relevant input data such as the pore size distribution and as such allows universal applicability. The advantage of the approach being advocated is also that it is very efficient and large reactor components can be modelled.
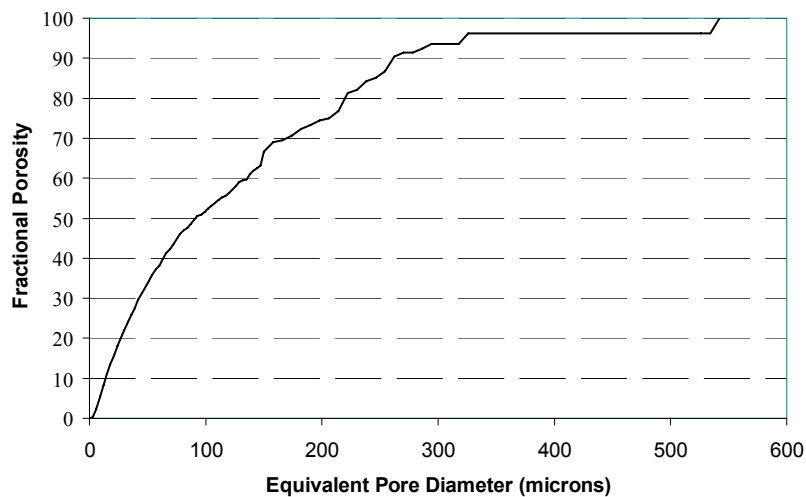
Figure 5: An example pore size distribution for an AGR moderator graphite.

As with any real microstructure, the pseudo-microstructure being generated contains a host of features such as calcination cracks within filler particles of different shapes (chosen randomly). The positioning of features is random (so long as the new feature does not break a rule such as increasing the pore volume between in a range of pore diameters). In terms of porosity, the code randomly chooses a location within the solid body, and a random pore size, and if permitted in line with the PSD & other rules, changes the values within the dynamic array to represent a void. The pores themselves are created using a method known as circle packing or circles within circles, as suggested by Weisstein (1999). At present, four diameter circles are used, as illustrated in Figure 6: D1 is the size of pore to be created and is the largest, then D2, D3 and finally D4. The diameters of the circles are found according to the ratio 1:0.3:0.22:0.14, respectively. The diameter of D1 is found using a random number generator picking numbers between the smallest and largest pore size when combined with the pore size distribution. Thus complex shapes are created using a hierarchical Boolean method. Initially the D2 pore is drawn then the component cycles through the D3 circles in contact with that circle and either draws or does not draw the touching circle according to a set probability. If the circle is drawn the component then steps to the D4 circles contacting the newly drawn D3 circle and repeats the operation. Once complete, the component moves to the next D3 circle and so on until all the circles have been visited. The method can produce highly complex shapes with varying aspect ratios as shown in Figure 7. Pores are allowed to overlap and over write to create interconnections. The solid areas seen within the pore, as shown in Figure 7 are not removed because the code is designed with 3D in mind and solid areas within pores may or may not be part of the solid.

Degradation

The degradation component is responsible for several tasks, but its primary role is to deplete the structure created by the microstructure component. To simulate radiolytic oxidation, a random location is chosen and then a complex logic statement is performed aimed at mimicking the morphological aspects of radiolytic oxidation so long as the random location is in a void (*i.e.* coolant gas) and within a mean free path of ~20 microns assuming pure CO_2 (Best *et al.*, 1985). In essence, this statement determines whether or not the value picked by the random number generator is at the edge of a pore or not. If the selection is appropriate, then the cell's value is modified to simulate oxidation into the pore wall, see Figure 8. This is repeated until a user defined porosity / weight loss value is reached. The effects do not have to be solely visual indeed any value within the multi-dimensional arrays can be dynamically modified to reflect simulated changes using a logic statement. Therefore, this component has been created with expansion at its core, by creating further logic statements and sub-routines other mechanisms such as neutron irradiation can be added and run separately or together (see later).
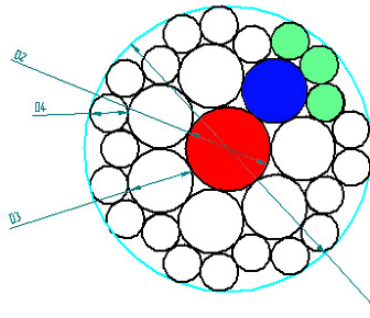

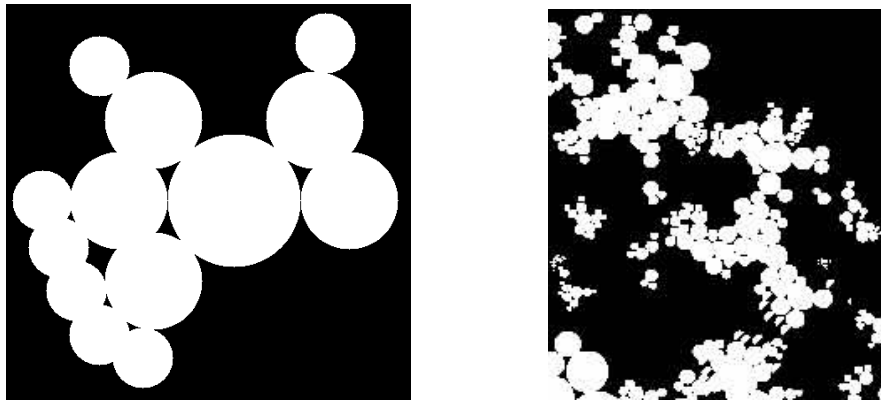**Figure 6**: Schematic of the method used to pack circles.

Figure 7: Enlarged images of a complex pore shape & network created using the circle packing method: black indicates solid and white indicates the pore.

Figure 8: Fine detail section of pores simulating the morphological effects of radiolytic oxidation.

Fracture

The fracture component of the code can be run independently from the degradation component. The component's task is to create a fracture path through the structure. The fracture method is not reliant upon predicted stress values at this time due to memory complications, however, it will still combine aspects of the ligament model, Steer (2003), Fictitious crack, Hillerborg *et al.* (1976) and the Crack Band Theory, Bažant and Oh (1983) to create a path through the structure, see Lynch and Neighbour (2004) for a detailed literature of fracture models. The algorithm that dictates the fracture path is heavily influenced by the surrounding microstructure and in essence takes the path of least resistance. The process is as follows:

1. Initial coordinate set for the break using a scan of one edge of the microstructure. The crack band will then be set.
2. Within the crack band there will be a scanning zone of the array. The zone will be scanned for the path of least resistance and minimum solid path, *i.e.* the path containing the weakest ligaments.
3. The cells alone the path will be removed or have their values modified.
4. The centre of the simulated FPZ then moves to a cell deemed most likely to fail next and the process repeated until there is a complete break.

Outputs

The outputs from the code are split distinctly between graphical (visual) and data files. The graphical output is handled using OpenGL 2.0. OpenGL enables the application to be expanded into 3D with relative ease. OpenGL is also less Central Processor Unit (CPU) intensive then other methods due to the Graphics Processor Unit (GPU) being able to take load off the CPU. The display method always for 32 bit depth colours and resizable windows, this means that any value entered in the array can be assigned a unique colour and any size array can be displayed. The image output can be saved to the computer's hard drive using a TGA file screen grab which saves the image without data loss. The data file output consists of the arrays created by the code during runtime. The subroutine can output both the microstructural array in full and the MLL array. The files are output in Comma Separated Value (CSV) format so the files can be imported directly into programs such as Microsoft Excel for further analysis and also to ensure the integrity of the array is kept intact. This means that the cell location within the CSV file directly corresponds to the cell location within the image file and within the array held in the computer's memory during runtime.

Random Number Generation

Random number generation is the key to success for the code's ability to generate usable microstructures and results, *i.e.* unbiased generation of locations & sizes of micro-structural features. Previous versions of the code were skewed because the code used a pseudo-random number generator based on the standard Microsoft RAND function (which is seeded with the CPU clock time). This method of number generation was found to produce the same sequence of numbers over and over because the random number function calls where occurring faster than the smallest time increment used to measure the CPU clock time. To solve the problem a class and new function was created using the mersenne twist developed by Matsumoto, M. and Nishimura, T. (1998). The mersenne twist is based upon the use of mersenne prime numbers to generate large bit depth number sequences which stream. In mathematics a mersenne prime number, M_n, is given by

$$M_n = 2^n - 1 \tag{2}$$

It is necessary for n to be prime for $2^n - 1$ to be prime. The class creates three simultaneous streams of numbers seeded by the CPU clock in milliseconds. Two of the streams are real numbers using floating 64-bit then forced to double integer range 1.7E +/- 308 (15 digits), the third stream is a 32 bit floating point number with a range 0 to $2^{32} - 1$. The three streams are then combined together to produce one number, which is rounded down to the nearest integer.

Results of Current Version

The new additions to the code allow for more analysis of the microstructure created, for example, the comparison of line porosity shown in Figure 9. This figure illustrates with increasing (radiolytic) porosity, a potentially bi-modal distribution which increases in line porosity as porosity increases. At lower levels of porosity, the two distributions overlap, but separate as the level of oxidation increases. This may be representative of the different classes of porosity and their prevalence to radiolytic attack. It should be noted that strictly Figure 9 plots MLL and not EPD, but the two measures have a close relationship. Further, it should be noted that some observations of higher than expected low strength failures in materials and components (*e.g.*, see Mirhabibi and Rand, 2007) have been attributed to a separate population of disparate flaws as opposed to a general background normal distribution of inherent flaw sizes (Steer, 2007). The fact that the model is able to support this view supports the approach being taken. Further, given that the output method means the line porosity can be plotted as raw data showing each row of cells porosity value (as it appears in the visual image, Figure 10) means it is easy to find the MLL, view the weaker areas of the microstructure, and ultimately predict the reduction of Young's modulus (or other properties) with oxidation, Figure 11. In this prediction, the curve at the moment is still too shallow in nature, and it is suggested this is due to the morphological aspects of the filler particles and the shape factors associated with the calcination cracks. In terms of the pseudo-microstructure generated, the impression is not dissimilar of that observed in thermally oxidised graphite to a similar weight loss, Figure 12.
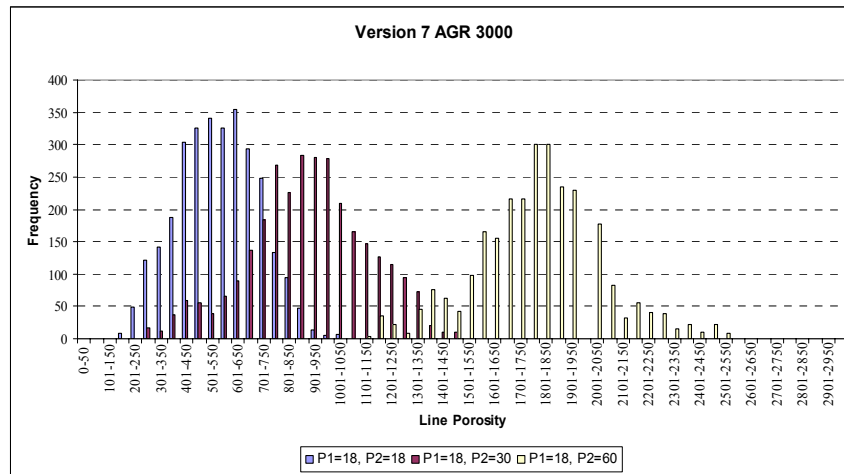

Figure 9: Comparison of the change in distribution of line porosity with increasing degradation in a [small] 3000x3000 cell model.
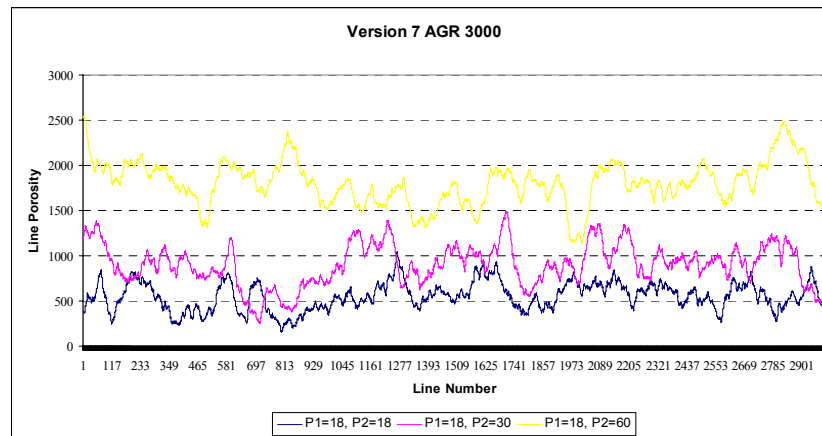

Figure 10: Comparison of actual line porosity within the simulated microstructure with increased porosity in a [small] 3000x3000 cell model.
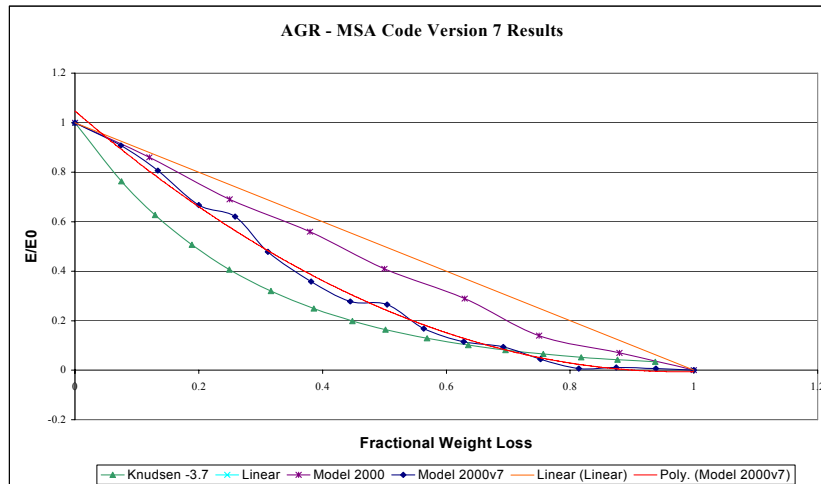
Figure 11: Comparison of the various developmental stage models against the ideal Knudsen relationship (Miller and Brocklehurst, 1988).
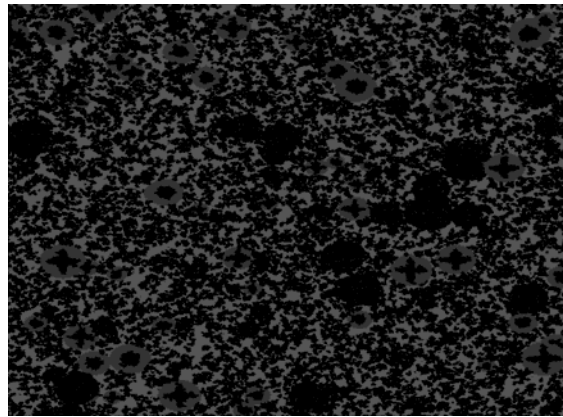

Figure 12: A simulated microstructure of 60% porosity, radiolytic oxidation graphite.

Summary and Conclusions

The application described in the paper aims to help provide a robust explanation for mechanical degradation and crack phenomena observed in AGR graphite moderator during operation. The design of the code has been detailed and its further development shown. The paper has included a brief description and explanation of the fracture process complications; a detailed explanation of how a simulated microstructure is created and degraded; and a process for which fracture will be included within the code (which is a hybrid of three fracture models previously used). The paper also presented a logic enabling better memory management and therefore allowing larger models to be created and run. The code presented has been shown to be capable of building all the elements of AGR moderator graphite microstructure including degradation mechanisms. Methods for the inclusion of further components and mechanisms, *e.g.* neutron irradiation, have been briefly discussed. The development of the code has been shown and compared to existing empirical models and shows some understanding in the trend found empirically with the Knudsen the relationship.

Acknowledgements

References

Allard, B., Rouby, D., Fantozzy, G., Dumas, D. and Lacroix, P. (1991). Fracture behaviour of carbon materials. *Carbon*, 29, 457-468.

Bažant, Z. P. and Oh, B. (1983). Crack band theory for fracture of concrete. *RILEM Material and Structures*, 16, 155-177.

Best, J. V., Stephens, W. J., and Wickham, A. J. (1985). Radiolytic graphite oxidation. *Progress in Nuclear Energy*, 16, [2], 127-178.

Birch, M., Schofield, P., Brocklehurst, J. E., Kelly, B. T., Harper, A. and Prior, H. (1990). The combined effects of fast neutron damage and radiolytic oxidation on the physical properties of Gilsocarbon graphite. *Carbon*, 90, 242-243.

Brocklehurst, J. E. (1977). Fracture in polycrystalline graphite. *Chemistry and Physics of Carbon*, 13, 145-279.

Brocklehurst, J. E., Brown, R. G., Gilchrist, K. E. and Labaton, V. Y. (1970). The effect of radiolytic oxidation on the physical properties of graphite. *Journal of Nuclear Materials*, 35, 183-194.

Burchell, T. D., Pickup I. M., McEnaney B., and Cooke R. G. (1985). The relationship between microstructure and the reduction of elastic modulus in thermally and radiolytically corroded nuclear graphites. *Carbon*, 24, [5], 545-549.

Fazluddin, S. B. (2002). R-curve behaviour in nuclear graphite materials. PhD Thesis. University of Leeds.

Hillerborg, A., Modeer, M. and Petersson, P. E. (1976). Analysis of crack formation and crack growth in concrete by means of fracture mechanics and finite elements. Cement and Concrete Research, 6, 773-782.

Lynch, C. and Neighbour, G. B. (2004). Modelling crack growth in complex heterogeneous brittle materials. First Year Progress Report, HULL/ENG/NUC/R009.

Lynch, C. and Neighbour, G. B. (2006). Development of a code to predict fundamental material and fracture properties of nuclear graphite. In:- "Extended Abstracts", International Conference on Carbon, "Carbon 2006", Aberdeen, U.K., 16-21 July 2006, ISBN 0-9553365-1-1 (Paper 6D3).

Matsumoto, M. and Nishimura, T. (1998). Mersenne twister: a 623-dimensionally equidistributed uniform pseudorandom number generator. *ACM Trans. Model. Comput. Simul.,* 8, [3].

Miller, W. N. and Brocklehurst, J.E. (1988). A statistical analysis of physical and mechanical property changes for graphite radiolytically oxidised in different coolants and recommended design rules for CAGR moderator and sleeve graphites. NRL-R-2009(S). AGR/GCWG/P(88)3.

Mirhabibi, A. R. and Rand, B. (2007). Graphite flake-carbon composites. II: fracture behaviour, toughness, notch sensitivity and Weibull modulus. *Carbon*, 45, 991-997.

Murdie, N., Edwards, I. A. S. and Marsh, H. (1986). Changes in porosity of graphite caused by radiolytic gasification by carbon dioxide. *Carbon*, 24, [3], 267-275.

Neighbour, G. B. and Hacker, P. J. (2001). The variation of compressive strength of AGR moderator graphite with increasing thermal weight loss. *Materials Letters*, 51, [4], 307-314.

Ouagne, P. (2001). Fracture property changes with oxidation and irradiation in nuclear graphites. PhD Thesis. University of Bath.

Rice, R. W. (1977). Microstructure dependence of mechanical behaviour of ceramics. In:- MacCrone (Editor), Treatise on Materials Science Technology, 11: Properties and Microstructure, 199-379, Academic Press, New York.

Rice, R. W. (1996a). Evaluation and extension of physical property-porosity models based upon minimum solid area. *Journal of Material Science*, 31, 102-118.

Rice, R. W. (1996b). Comparison of physical property-porosity behaviour with minimum solid area models. *Journal of Materials Science*, 31, 1509-1528.

Rice, R. W. (1996c). The porosity dependence of physical properties of materials: a summary review. *Key Engineering Materials*, 115, 1-20.

Sakai, M., Urashima, K., and Inagaki, M. (1983). Energy principle of elastic-plastic fracture and its application to the fracture mechanics of polycrystalline graphite. *Journal of the American Ceramic Society*, 66, 868-874.

Steer, A. G. (2003). A structural approach to the description and determination of its physical properties. Private communication.

Steer, A. G. (2007). Private Communication.

Weisstein, E. W. (1999). "Circle packing". From MathWorld - A Wolfram Web Resource. http://mathworld.wolfram.com/CirclePacking.html, CRC Press LLC, accessed January 15th 2006.